Available online at www.sciencedirect.com
ScienceDirect
International Journal of Thermal Sciences 47 (2008) 1647–1657
International Journal of Thermal Sciences
www.elsevier.com/locate/ijts

Combined laminar natural convection and surface radiation heat transfer in a modified cavity receiver of solar parabolic dish

K.S. Reddy *, N. Sendhil Kumar

Heat Transfer and Thermal Power Laboratory, Department of Mechanical Engineering, Indian Institute of Technology Madras, Chennai 600 036, India

Received 3 August 2007; received in revised form 1 November 2007; accepted 4 December 2007

Available online 9 January 2008

Abstract

The numerical study of combined laminar natural convection and surface radiation heat transfer in a modified cavity receiver of solar parabolic dish collector is presented in this paper. A two-dimensional simulation model for combined natural convection and surface radiation is developed. The influence of operating temperature, emissivity of the surface, orientation and the geometry on the total heat loss from the receiver is investigated. The convective heat loss from the modified receiver is significantly influenced by the inclination of the receiver whereas the radiation heat loss is considerably affected by surface properties of the receiver. The Nusselt number correlations are proposed separately for both natural convection and surface radiation based on large set of numerical data for a given range of parameters of practical interest. It is observed that the convection and radiation heat losses are found respectively 52% and 71.34% of the total heat loss at 0° inclination and 40.72% and 59.28% at 90° inclination for the modified cavity receiver with an area ratio of 8 and 400 °C. The convection and radiation numerical procedure is validated with other models. The results obtained from the present numerical procedure are in reasonable agreement with other well-known open cavity models.

Keywords: Modified cavity receiver; Solar parabolic dish collector; Natural convection; Surface radiation; Nusselt number

1. Introduction

Combined natural convection and radiation exchange between surfaces involving a radiatively non-participating medium (air) occur in several engineering applications such as solar energy collection devices, energy efficient buildings, and double pane window. The solar parabolic dish collector is known as most efficient system among solar thermal devices. The solar parabolic dish collector maintains its optical axis always pointing directly towards the sun. The geometry of the concentrator allows reflecting the incident solar rays onto the receiver, which is located at the focal plane of the collector. During its rotation, the receiver experiences change in the complete behavior of the fluid and the heat transfer characteristics. The orientation of the receiver might alter the thermal performance of solar parabolic dish system. The estimation of heat losses from the receiver is an important input to the performance evaluation of the solar dish collector. The natural convection and radiation heat losses from the receiver substantially reduce the performance of the system. A moderate temperature rise leads to a considerable heat loss, which may directly influence the performance of dish system. Therefore, the effect of combined natural convection and surface radiation on total heat loss needs to be investigated.

Experimental and numerical investigations on natural convection heat transfer in open cavities and enclosures have carried out by earlier researchers [1–3]. An analytical model was presented for estimation of convective heat loss of a large cubical cavity receiver based on inside local heat transfer coefficient and interaction of air through the aperture due to buoyancy and wind effects [4]. Experimental Nusselt number correlations for isothermal open cubical cavity for different angles of inclination were presented by LeQuere et al. [5]. A simple model for the convective heat transfer from a solar cavity receiver based on the results of experimental studies of cubical cavities was presented by Siebers and Kraabel [6]. Subsequently McDonald [7] modified the model for a cylindrical shaped frustum receiver incorporating aperture size, surface temperature and receiver angle. Leibfried and Ortjohann [8] studied the natural convec-

* Corresponding author. Tel.: +91 44 22574702; fax: +91 44 22574652, 22570509.
E-mail address: ksreddy@iitm.ac.in (K.S. Reddy).

1290-0729/$ – see front matter
doi:10.1016/j.ijthermalsci.2007.12.001

Nomenclature

A_1	Focal image / aperture area of the receiver	m^2
A_w	Heat transfer area of the inner receiver surface	m^2
A_i	Area of surface i	m^2
A_j	Area of surface j	m^2
D	Cavity diameter of the receiver	m
d	Aperture diameter of the receiver	m
E_i	Emissive power of surface i	
F_{ji}	View factor between surface j and surface i	
Gr	Grashof number	
h_C	Convective heat transfer coefficient	$W/(m^2\,K)$
h_R	Radiative heat transfer coefficient	$W/(m^2\,K)$
k_f	Thermal conductivity of the working fluid	$W/(m\,K)$
Nu_R	Radiative Nusselt number	
Nu_C	Convective Nusselt number	
N_{rc}	Radiation–conduction number	
Pr	Prandtl number	
P_{atm}	Atmospheric pressure	
Ra	Rayleigh number	
S2S	Surface-to-Surface	
T_w	Surface wall temperature	K
T_∞	Ambient temperature	K
$q_{out,i}$	Energy flux leaving the surface	W/m^2
$q_{in,i}$	Energy flux incident on the surface from the surrounding	W/m^2
q	Velocity vectors (r, ϕ, θ)	
Q_C	Convective heat loss	W
Q_R	Radiative heat loss	W
Q_{Total}	Total heat loss	W
X	Body force per unit volume	

Greek symbols

θ	Angle of inclination of receiver, degree	
υ	Kinematic viscosity of the fluid	m^2/s
ρ	Density of the fluid	kg/m^3
ε_i	Emissivity of surface i	
ε_{c1}	Emissivity of the receiver surface	
σ	Stefan–Boltzmann's constant (5.67×10^{-8} $W/m^2\,K^4$)	
δ_{ij}	Kronecker delta	
∇	Laplace operator	

Subscripts

C	Convection
R	Radiation
i, j	Surfaces

tion heat loss in electrically heated spherical and hemispherical receivers. Taumoefolau et al. [9] investigated the natural convection heat loss from an electrically heated model cavity receiver for different inclinations varying from $\theta = -90°$ (cavity facing up) to $\theta = +90°$ (cavity facing down) with temperature ranging from 450 °C to 650 °C. The phenomenon of existing of natural convection heat loss at 90° inclination of the receiver was observed through their numerical and experimental studies, which contradict with other heat loss models. Paitoonsurikarn and Lovegrove [10] presented a refined, Nusselt number correlation based on the numerical simulation results of three different cavity geometries (model receiver, 20 m^2 dish receiver and 400 m^2 dish receiver). Sendhil and Reddy [11] carried out a comparative study of cavity, semicavity and modified cavity receivers for solar dish concentrator. Sendhil and Reddy [12] developed the 2D natural convection heat loss model for modified cavity receiver of two different configurations. Natural convection heat loss is observed at 90° inclination of the receiver for both the receiver.

Some studies have been reported on combined effect of natural convection and surface radiation in an open cavity in the literature. Lage et al. [13] numerically analyzed natural convection and radiation in a 2D cavity with open-end and extended simulations to an ash hopper. Lin et al. [14] investigated the effect of surface radiation on turbulent free convection in a cavity open at the side. Balaji and Venkateshan [15] reported the numerical results of the fundamental problem of interaction of surface radiation with laminar free convection in an open cavity with air as the intervening medium. The surface radiation alters the basic flow pattern as well as overall thermal performance of the open cavity. Balaji and Venkateshan [16] numerically studied the combined conduction, natural convection and radiation heat transfer in a vertical slot (closed end open cavity). Dehghan and Behnia [17] analyzed numerically and experimentally the combined natural convection, conduction and radiation heat transfer in a discretely heated open top cavity. A comparison of the numerical and experimental observations showed that the accurate prediction of the flow and thermal field influenced by radiation heat transfer. Ramesh and Merzkirch [18] carried out an experimental study for the combined natural convection and radiation heat transfer in a cavity with top opening. The flow and temperature patterns were significantly influenced by emissivity of the cavity wall. Singh and Venkateshan [19] discussed a numerical study of combined laminar natural convection and surface radiation heat transfer in a 2D side vented open cavity for different aspect ratios, sidevent ratios and surface emissivities using air as the working fluid. Based on numerical data, separate Nusselt number correlations have been developed for convective and radiative heat transfer. Hinojosa et al. [20] presented the numerical results of the heat transfer by natural convection and surface thermal radiation in a titled 2D open cavity. The inclination of the cavity receiver influences significantly the convective Nusselt number whereas no influence on radiation Nusselt number. Bouali et al. [21] studied numerically the effects of surface radiation and inclination angle on heat transfer and flow structures in an inclined rectangular enclosure with a centered inner body. Balaji and Venkateshan [22] developed separate correlations for both convective and radiative heat transfer in a square cavity with air as the intervening medium. The effects of inclination

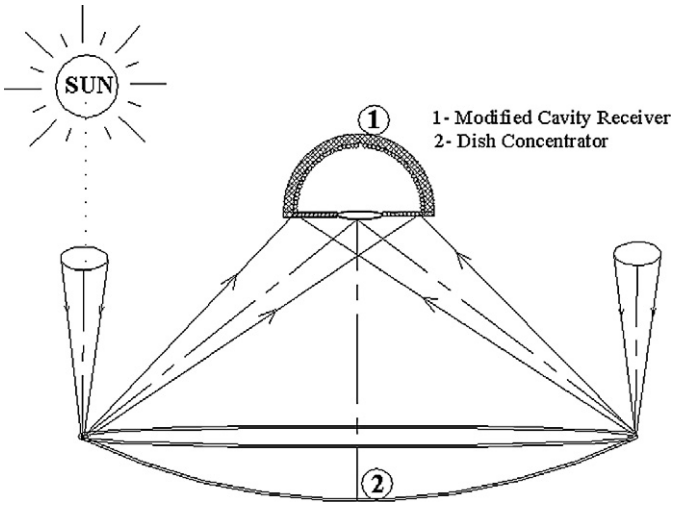

Fig. 1. Solar parabolic dish collector.

and emissivity of the receiver on combined natural convection and surface radiation heat transfer was investigated by Sendhil and Reddy [23]. The earlier studies were focused only on simple geometries of the open cavity. Most of the studies were dealt with the heat transfer from receiver at fixed inclinations. In the present study, a 2D numerical model with steady-state combined laminar natural convection and surface radiation heat transfer from a modified cavity receiver (hemispherical) of a solar parabolic dish system for various orientations has been developed.

2. Modelling of modified cavity receiver

2.1. Combined convection and surface radiation model

The modified cavity receiver for solar parabolic dish systems is a cavity type receiver with small opening at the aperture through which concentrated sunlight enters. Usually the receiver is mounted at the focal point of the solar parabolic dish collector. The assembly of the solar parabolic dish with modified cavity receiver is shown in Fig. 1. The modified cavity receiver made of copper tubing. The copper tubes are wound spirally around to get the respective shape (hemispherical) of the receiver (Fig. 2). The outer surface of the receiver is covered with opaque insulation of 20 mm thickness to reduce the heat losses. The working fluid inside the cavity is air, and the Prandtl number of the fluid is considered as 0.71. The temperature of the fluid is assumed same as that of the inner surface temperature.

The flow and heat transfer simulations were based on the simultaneous solution of the system of equations describing the conservation of mass, momentum and energy. The vector form of continuity, momentum and energy equations can be expressed as [24]:

- Continuity equation

$$\nabla \cdot q = 0 \tag{1}$$

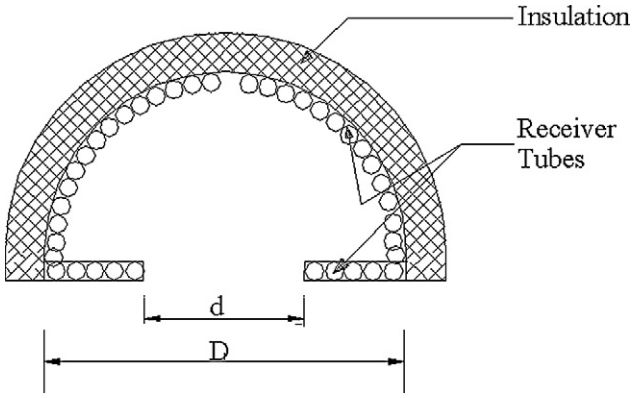

Fig. 2. Schematic of modified cavity receiver.

- Momentum equation

$$q \cdot \nabla q = X - \frac{\nabla p}{\rho} + v\nabla^2 q \tag{2}$$

- Energy equation

$$\nabla \cdot (k_f \nabla T) = 0 \tag{3}$$

The continuity, momentum and energy equations are used to solve for laminar natural convection model. To account for the radiation exchange in an internal surface of the modified cavity receiver along with the natural convection heat loss, S2S model is chosen in the present numerical procedure. The S2S model is coupled with the laminar natural convection model. In the S2S radiation model, the surfaces are taken as gray and diffuse. The emissivity and absorptivity of a gray surface are independent of the wavelength. For a diffuse surface, the reflectivity is independent of the outgoing (or incoming) directions. The energy exchange between two surfaces depends on their size, separation distance, and orientation. The influences of these parameters are accounted by a view factor. The main assumption of the S2S model is that the absorption, emission, scattering of radiation by the working fluid have not considered. Therefore, only "surface-to-surface" radiation is considered for the analysis. The emissivity of the internal cavity surface was varied from zero to unity to predict the effects of combined natural convection and surface radiation on total heat transfer. The radiant flux from a given surface consists of directly emitted and reflected energy. The reflected energy flux is dependent on the incident energy flux from the surroundings, which then can be expressed in terms of the energy flux leaving all other surfaces. The energy reflected from surface i is given by [25]:

$$q_{\text{out},i} = \varepsilon_i \sigma T_i^4 + (1 - \varepsilon_i) q_{\text{in},i} \tag{4}$$

The amount of incident energy upon a surface from another surface is a direct function of the surface-to-surface "view factor", F_{ji}. The incident energy flux $q_{\text{in},i}$ can be expressed in terms of the energy flux leaving all other surfaces as [25]:

$$A_i q_{\text{in},i} = \sum_{j=1}^{N} A_j q_{\text{out},j} F_{ji} \tag{5}$$

For N surfaces, view factor reciprocity theorem gives

$$A_j F_{ji} = A_i F_{ij} \tag{6}$$

Therefore $q_{\text{in},i}$ is expressed as:

$$q_{\text{in},i} = \sum_{j=1}^{N} F_{ij} q_{\text{out},j} \tag{7}$$

Substituting Eq. (7) in Eq. (4), we have:

$$q_{\text{out},i} = \varepsilon_i \sigma T_i^4 + (1-\varepsilon_i) \sum_{j=1}^{N} F_{ij} q_{\text{out},j} \tag{8}$$

Eq. (8) can be re-written as:

$$J_i = E_i + (1-\varepsilon_i) \sum_{j=1}^{N} F_{ij} J_j \tag{9}$$

Also,

$$J_i - (1-\varepsilon_i) \sum_{j=1}^{N} F_{ij} J_j = E_i \tag{10}$$

$$\sum_{j=1}^{N} \big(\delta_{ij} - (1-\varepsilon_i) F_{ij}\big) J_j = E_i \tag{11}$$

where

$$\delta_{ij} = \begin{cases} 1 & \text{when } i = j \\ 0 & \text{when } i \neq j \end{cases}$$

The radiosity equation is expressed in vector form as:

$$K J = E \tag{12}$$

where K is an $N \times N$ matrix, $K = (\delta_{ij} - (1-\varepsilon_i) F_{ij})$, J is the radiosity vector, and E is the emissive power vector.

2.2. Boundary conditions

The geometry of the receiver was subjected to various types of boundary conditions. The internal receiver surfaces are continuously exposed to solar flux. Because of this, the internal surface area may attain uniform isothermal condition at the point of stagnation condition. Therefore, the isothermal boundary condition was given to the inner receiver walls. To prevent heat loss from the receiver, the outer surface of the receiver was covered with insulating material of ceramic wool. Therefore, in modeling, the outer walls of the receiver were treated as adiabatic. The receiver is exposed to ambient, air can enter into the receiver from all the directions. Hence, pressure inlet boundary condition was applied to the outer domain.

2.2.1. Isothermal boundary condition:

The inner regions (surfaces 2, 3, 4 in Fig. 2) of the modified cavity receiver are taken as constant temperature. The corresponding boundary condition for isothermal surface is:

$$T = T_w$$

2.2.2. Pressure inlet boundary condition:

The outer domain is treated to be a pressure inlet boundary condition. So boundary condition would be:

$$P = P_{\text{atm}}$$

2.2.3. Adiabatic boundary condition:

The outer surface (surface 1 in Fig. 1) of the modified cavity receiver is treated to be adiabatic and the corresponding boundary condition would be:

$$\frac{\partial T_w}{\partial \phi} = 0$$

The following assumptions have been taken to solve the combined natural convection and surface radiation of modified cavity receiver.

(a) The temperature of the fluid is same as the surface temperature.
(b) The internal surfaces of the receiver are gray and diffuse.

2.3. Numerical procedure

The receiver geometry is hemispherical and all the surfaces are covered with tubing. The present study requires 3D analysis of the modified cavity receiver. Separate 2D and 3D simulations were carried out at 90° inclinations of the receiver. It was found that the 3D simulations predict only 2.6% better than that of the 2D simulations. For other inclinations (<90°), the predictions would deviate about an average deviation of 14.5%. However, the computational time and grid size involved in 3D are respectively 5 times and 15 times higher than 2D. Therefore, a 2D model has been adopted in the present study to predict the total heat loss from the receiver with little approximation.

The 2D modeling and grid generation was carried out in the GAMBIT 2.0.4 package. In reality, an infinite atmosphere surrounds the modified cavity receiver. To model this condition, the size of the enclosure (outer domain) was increased until it had an insignificant effect on the working fluid and heat flow near the receiver. This condition was achieved, when the diameter of the enclosure (outer domain) is about thirty times the diameter of the receiver. The grid independence study was carried out with fine grid size of 12,673 nodes inside the cavity receiver and coarse grid size of 185×185 nodes near the outer domain. The computational grid and boundary conditions of the modified cavity receiver are shown in Fig. 3. The laminar natural convection model equations and radiosity vector equations were solved using the software package FLUENT 6.1. In this model, 2D governing equations with laminar, incompressible and steady state problem were solved using an implicit solver. Boussinesq approximation was considered while solving the momentum equation. The average radiative heat flux leaving from the internal surface of the modified cavity receiver is obtained directly from the FLUENT results. The properties of the working fluid were taken based on the average temperature of the receiver surface and the ambient air. For pressure velocity coupling, SIMPLEC algorithm was used with first order upwinding scheme for the discretization of equations. A convergence criterion of 10^{-3} was imposed on the residuals of the continuity and momentum equations. The convergence criterion of 10^{-6} was given on the residual of energy equation.

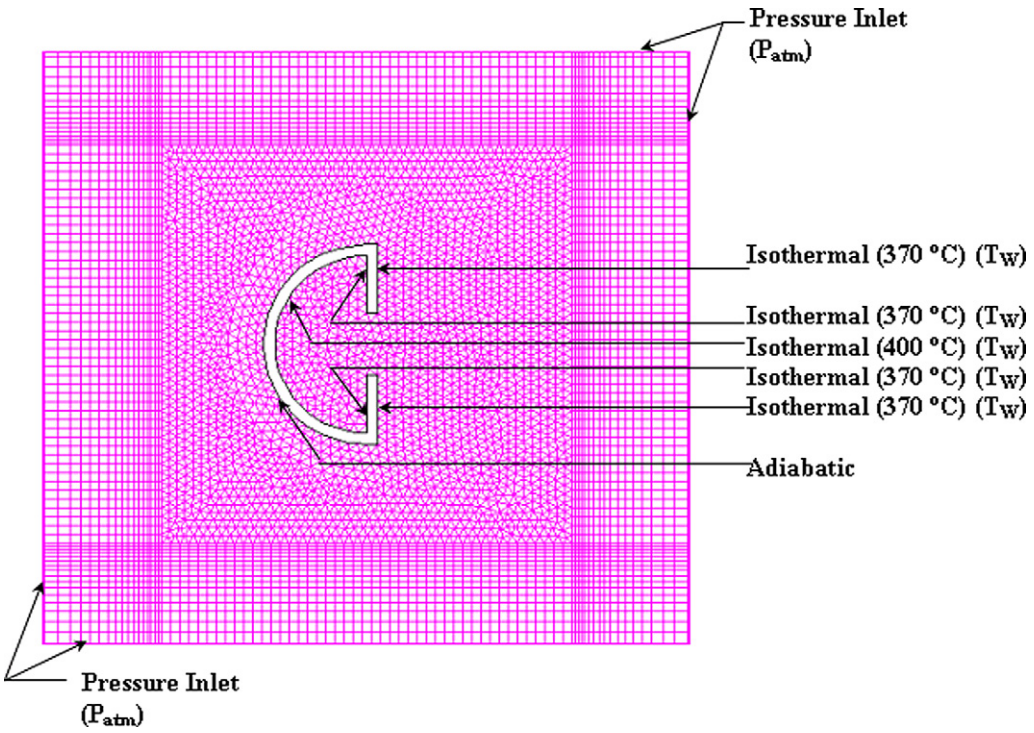

Fig. 3. Computational grid and boundary conditions of the modified cavity receiver.

3. Validation of the numerical procedure

The geometries considered in the present study are relatively new and no experimental data is available for similar geometry. The numerical procedure is validated for the hemispherical enclosure and open cavity square cavity geometries and subsequently adopted here.

3.1. Natural convection in hemispherical enclosure

The experimental work reported by Yasuaki et al. [1] has been considered for validating the numerical procedure. The hemispherical geometry considered for validation is shown in Fig. 4. The hemispherical enclosure problem was experimentally studied under steady state, laminar conditions. The curved portion and bottom surface were taken as cold and hot surfaces respectively. The isotherms of the hemispherical enclosure are shown in Fig. 5.

The experimental Nusselt number correlation for different Rayleigh number (Ra) and Prandtl number (Pr) was given by Yasuaki et al. [1];

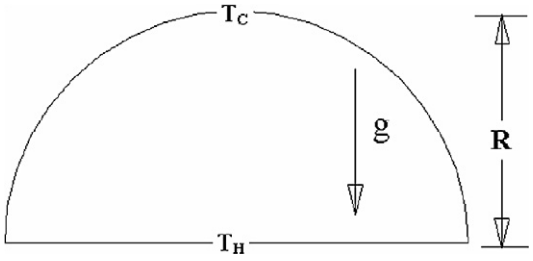

Fig. 4. Schematic of hemispherical enclosure with boundary conditions.

$$Nu_C = 0.185Ra^{0.25} \quad (10^6 \leqslant Ra \leqslant 6\times10^{10} \text{ and } 6 \leqslant Pr \leqslant 13000) \tag{13}$$

To validate the experimental correlation, we (present authors) proposed a Nusselt number correlation in the same form using water as working fluid ($Pr = 6.3$),

$$Nu = 0.176Ra^{0.253} \ (10^5 \leqslant Ra \leqslant 10^7) \tag{14}$$

The geometry of hemispherical enclosure has been created in the Gambit 2.0.4. The simulations have been carried out using the CFD package FLUENT 6.1. For different operating conditions, the area weighted average Nusselt numbers of hot surface of the hemispherical enclosure have been obtained for different Rayleigh numbers (Table 1).

The comparison of the present numerical procedure with that of the experimental case of Yasuaki et al. [1] for a hemispherical enclosure is illustrated in Table 1. It is observed that present numerical procedure is reasonable agreement with the experimental data within ±5% deviation.

Table 1
Validation of the numerical procedure for natural convection heat loss

Rayleigh number (Ra)	Nusselt number (Nu_C)		Percentage of deviation
	Yasuaki et al. [1]	Present work	
2.7763×10^5	4.25	4.31	−1.41
1.9437×10^6	6.91	6.57	4.92
2.8523×10^6	7.60	7.34	3.42
4.9288×10^6	8.72	9.10	−4.35
7.8266×10^6	9.78	10.00	−2.25
2.2818×10^7	12.79	12.92	−1.01
1.1683×10^7	10.82	10.68	1.29

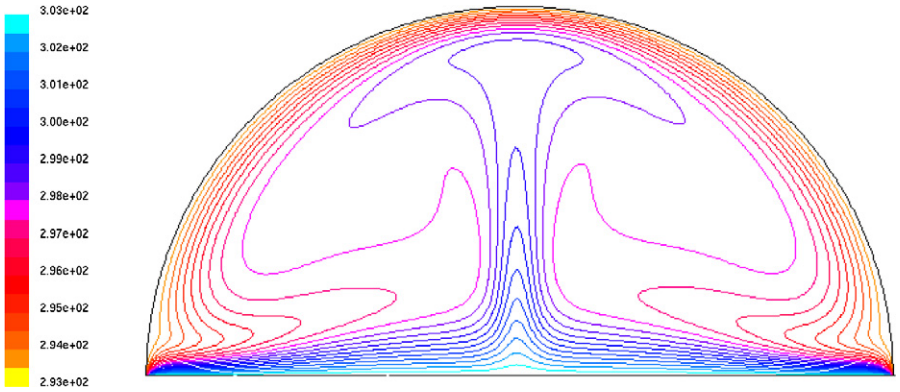

Fig. 5. Temperature contours of hemispherical enclosure.

Table 2
Convection and radiation Nusselt numbers for open cavity model ($\varepsilon = 1$)

Grashof number	Parameters	Open cavity [15]	Present numerical procedure	Percentage of deviation
6.301×10^6	Nu_R	23.68	22.88	3.37%
	Nu_C	21.00	20.57	2.04%
5.562×10^6	Nu_R	24.52	23.41	4.52%
	Nu_C	20.02	19.49	2.65%

3.2. Combined natural convection and surface radiation in open cavity

With a view to validate the combined laminar natural convection and the surface radiation in a modified cavity receiver, the open cavity with an aspect ratio of 2 and temperature ratio (T_∞/T_w) of 0.75 and 0.8 has been considered. The convective and radiative Nusselt numbers were proposed for an open cavity for the Grashof number of 6.301×10^6 and 5.562×10^6. The numerical procedure in terms of Nusselt number for open cavity was compared with Balaji and Venkateshan [15]. The numerical results obtained were in good agreement (4.5% deviation) with Balaji and Venkateshan [15] model (Table 2).

4. Results and discussions

The natural convection and surface radiation heat losses from the modified cavity receiver were estimated for different inclinations and temperatures. A 2D numerical analysis of receiver was carried out for positive inclination (θ) angles of 0 (cavity aperture facing sideways) to 90° (cavity aperture facing down). The combined natural convection and surface radiation heat loss from the receiver was studied for various temperatures ranging from 300 °C to 700 °C. The temperature contours in the receiver at 400 °C for $\varepsilon = 0$ and $\varepsilon = 1$ at different inclinations are respectively shown in Figs. 6 and 7.

The natural convective currents occupy most of the receiver for $\varepsilon = 0$, at $\theta = 0$ inclination. The hot air (stagnant zone) lies at the top portion of the receiver aperture. As the receiver inclination changes from 0 to 90°, the stagnant zone gradually increases in the receiver. At receiver inclination 90°, the entire cavity is filled with a stagnant zone. Increasing the stagnant air zone in the receiver decreases the convective heat loss from 0 to 90°. The maximum convection heat loss occurs at $\theta = 0$ and decrease gradually to 90°. For $\varepsilon = 1$, the radiation heat transfer influence the air temperature in the receiver which in turn enhances the convection heat loss. In addition, the convection heat loss decreases from 0 to 90°. Thus, the convective heat loss changes substantially with the inclination of the cavity receiver, whereas the radiation heat loss is remains constant for all inclinations of the modified cavity receiver. The average heat transfer coefficients and Nusselt numbers were determined based on a large set of numerical data (200 data points). Correlations for average convection Nusselt number (Nu_C) and radiative Nusselt number (Nu_R) have been developed for a working fluid of air, whose Prandtl number (Pr) is 0.71.

The convective Nusselt number (Nu_C) is given as:

$$Nu_C = 0.534 Gr_D^{0.218} (1+\cos\theta)^{0.916} (1+\varepsilon)^{0.473} \times \left(\frac{N_{\rm rc}}{N_{\rm rc}+1}\right)^{1.213} (T_R)^{0.082} \left(\frac{d}{D}\right)^{0.099} \quad (15)$$

The radiative Nusselt number (Nu_R) is given as

$$Nu_R = 9.650 Gr_D^{0.068} (1+\cos\theta)^{0.001} (\varepsilon)^{0.546} (N_{\rm rc})^{0.478} \times \left[1-(T_R)^4\right]^{8.768} \left(\frac{d}{D}\right)^{0.493} \quad (16)$$

where radiation–conduction number ($N_{\rm rc}$) is given as:

$$N_{\rm rc} = \frac{\sigma T_w^4 (\frac{D}{2})}{(T_w - T_\infty) k_f}$$

and temperature ratio (T_R) is

$$T_R = \frac{T_\infty}{T_w}$$

The convective heat transfer coefficient can be expressed as:

$$h_C = \frac{Nu_C \times k_f}{D} \quad (17)$$

The convective heat loss from the modified cavity receiver is given as:

$$Q_C = h_C \times A_1 \times (T_w - T_\infty) \quad (18)$$

Similarly, the radiative heat transfer coefficient and its corresponding heat loss can be written as:

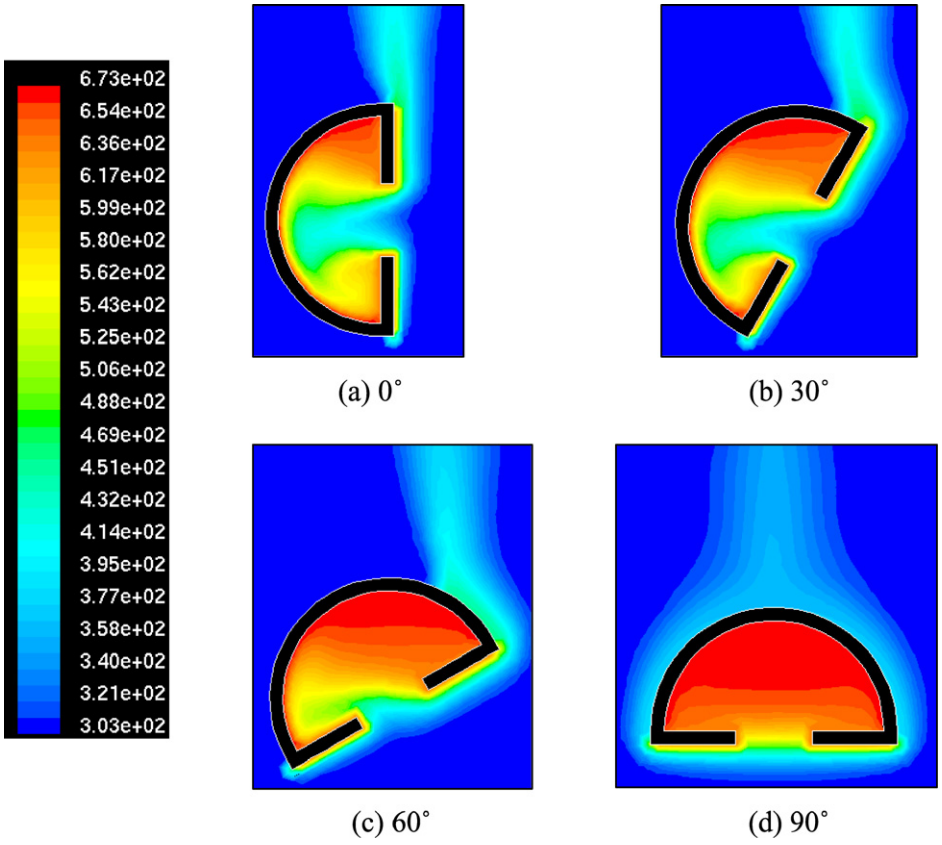

Fig. 6. Temperature contours of the modified cavity receiver at 400 °C and $\varepsilon = 0$.

$$h_R = \frac{Nu_R \times k_f}{D} \tag{19}$$

$$Q_R = h_R \times A_1 \times (T_w - T_\infty) \tag{20}$$

The total heat loss from the modified cavity receiver can be expressed as:

$$Q_{\text{total}} = Q_C + Q_R \tag{21}$$

Range of parameters

$$10^6 \leqslant Gr_D \leqslant 10^7; \quad 0 \leqslant \theta \leqslant 90^\circ$$

(in steps of positive angle of 15°);

$$0.3 \leqslant \frac{d}{D} \leqslant 0.4; \quad 0.53 \leqslant T_R \leqslant 0.33$$

$$0 \leqslant \varepsilon \leqslant 1; \quad 38 \leqslant N_{\text{rc}} \leqslant 175$$

These correlations are function of Grashof number (Gr), angle of inclination (θ), radiation–conduction number (N_{rc}), temperature ratio (T_∞/T_w), surface emissivities (ε) and diameter ratio (d/D). The model includes both convection and radiation heat transfer. Therefore, the Grashof number has been included in the Nusselt number correlations. The effect of Grashof number on the radiative heat loss is negligibly small, which is reflected in the exponent. The exponent of angle of inclination (θ) in the convective Nusselt number correlation is higher than that of the radiative Nusselt number correlation. This shows that the convective Nusselt number is more dependent on the inclination of the receiver. The term radiation–conduction number (N_{rc}), a superfluous parameter if only one fluid is considered. Near to the receiver surface, the working fluid (air) becomes stagnant. In order to bring the effect of conduction (stagnant) on the combined heat loss, thermal conductivity of the fluid (k_f) is considered in the N_{rc} term. In evolving the above correlation, $(1 + \cos\theta)$ has been used as the appropriate form for (θ), because, even $\theta = 90°$, Nusselt number would be non-zero. Similarly, $(1 + \varepsilon)$ has been used in the same form in Eq. (15) to avoid zero convective Nusselt number at $\varepsilon = 0$. As ε increases, radiative Nusselt number increases and hence the power law form is used for an emissivity term. The radiative flux depends on fourth power of the surface temperature. Hence, the present form $[1 - (T_R)^4]$ is used. The parity plots for radiation and convection Nusselt number are shown in Figs. 8 and 9 respectively. High correlation coefficients of 0.988, 0.982 and a standard error of 0.1098, 0.067 indicate the goodness of fit for both convective and radiative Nusselt number. The variation of convective and radiative heat losses with the inclination of the modified cavity receiver at $\varepsilon = 0$ and $\varepsilon = 1$ are shown in Fig. 10. The convection heat loss at $\varepsilon = 1$ is higher than the convection heat loss at $\varepsilon = 0$. This is mainly due to the inclusion of the radiation heat transfer in the convection model. Inclusion of radiation alters the basic flow pattern in the modified cavity receiver, which in turn affects the convective heat transfer coefficient [15]. The augmented flow pattern at $\varepsilon = 1$ increases the convective heat transfer coefficient. Therefore, radiation enhances the convective heat transfer.

The variation of surface radiation with emissivity of the surface has been studied. It is observed that a sharp increase in

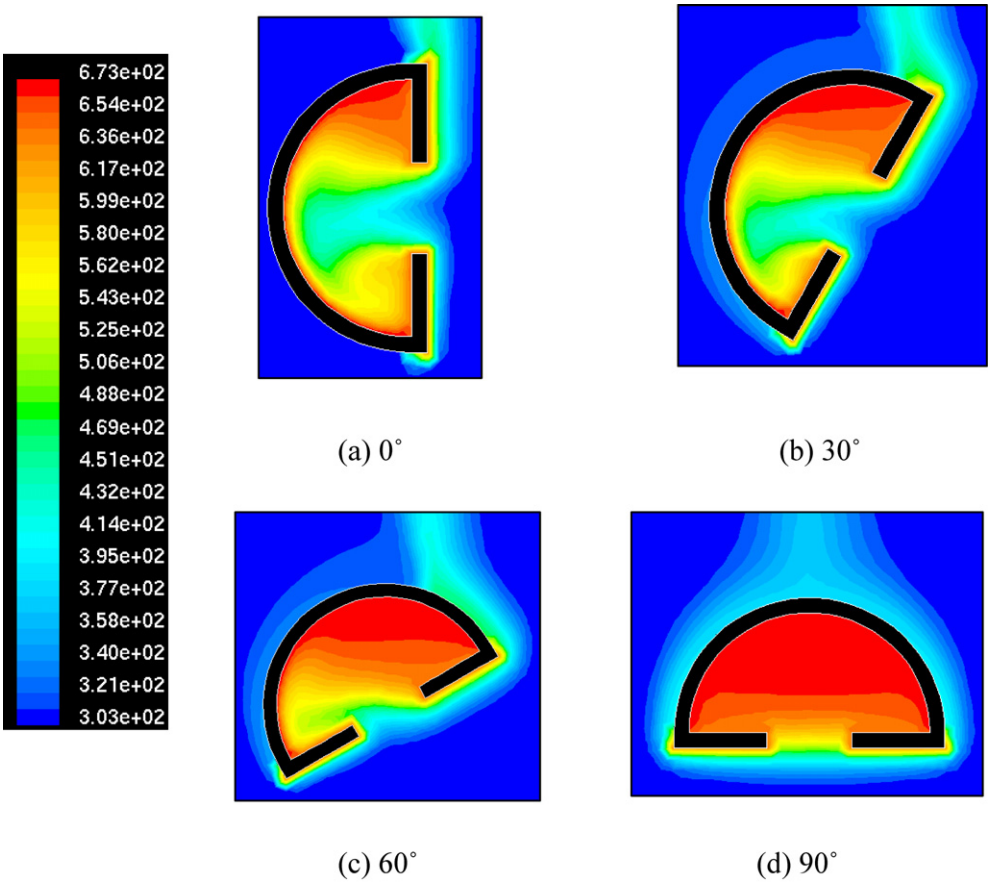

Fig. 7. Temperature contours of the modified cavity receiver at 400 °C and $\varepsilon = 1$.

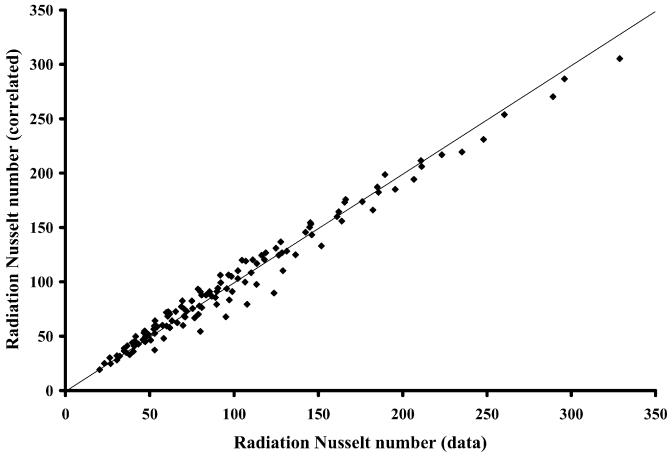

Fig. 8. Parity plot of radiation Nusselt number of modified cavity receiver.

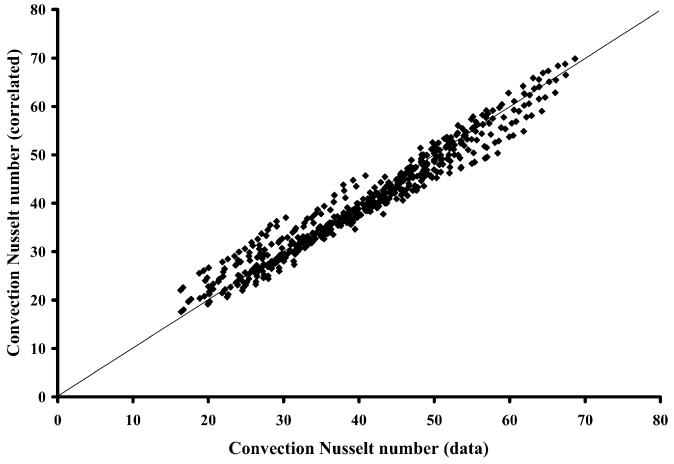

Fig. 9. Parity plot of convection Nusselt number of modified cavity receiver.

radiative Nusselt number with the emissivity of the receiver. In contrast, a slight variation was observed in the convection Nusselt number with the emissivity of the receiver. The emissivity of the surface has direct influence on the surface radiation; which, in turn increases the radiation and convection Nusselt number. The variation of convective and radiative Nusselt number with the emissivity of the modified cavity receiver of surface temperature of 400 °C for an area ratio (A_w/A_1) of 8 is shown in Fig. 11.

The variation of radiation Nusselt number with inclination of the receiver has been carried out numerically for different area ratios. The radiation Nusselt number is independent of the inclination of the receiver, whereas it is dependent on area ratio. The total heat loss is a combined heat loss of natural convection and surface radiation. The quantification of convection and surface radiation heat transfer at 400 °C and $\varepsilon = 1$, for various area ratio and receiver inclinations are illustrated in Table 3. It is observed that at 0° inclination of the modified

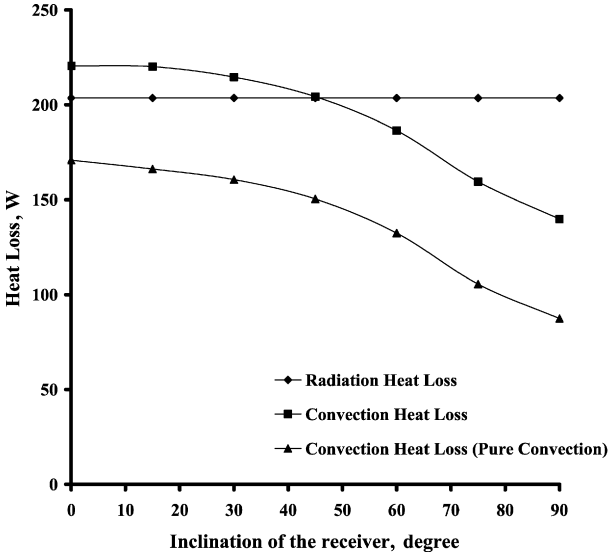

Fig. 10. Variation of heat loss with the inclination of the modified cavity receiver.

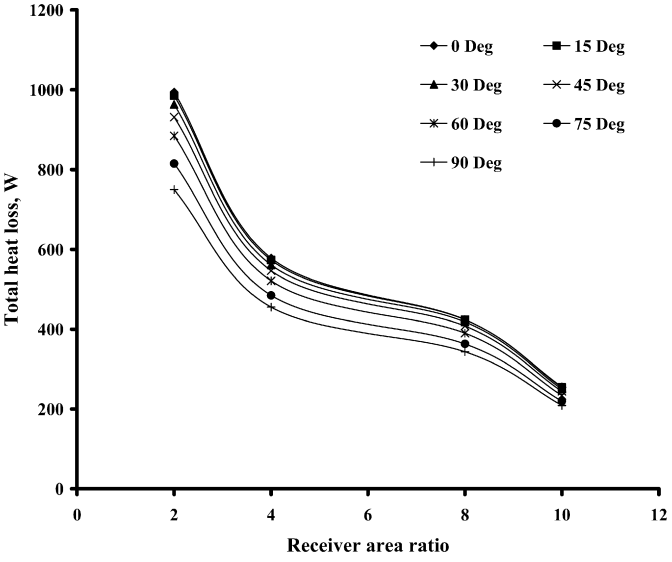

Fig. 12. Effect of area ratio on total heat loss from the modified cavity receiver.

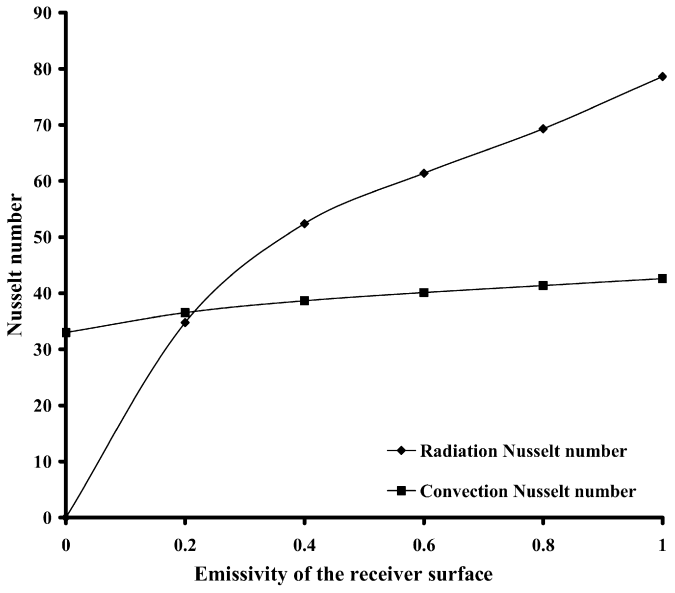

Fig. 11. Variation of Nusselt number with the emissivity of the receiver surface.

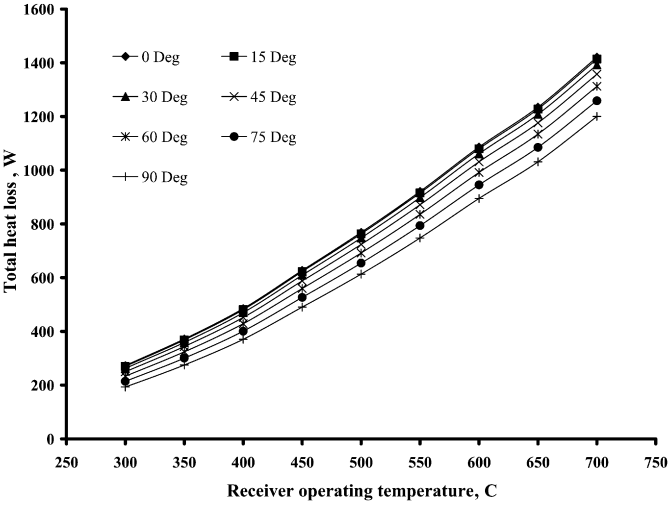

Fig. 13. Effects of operating temperature on total heat loss of the modified cavity receiver.

cavity receiver of area ratio of 8, the convection and radiation heat losses are 52% and 71.34% of the total heat loss and for 90° inclination; it is 40.72% and 59.28% of the total heat loss.

The effect of area ratio (A_w/A_1) on total heat loss has been investigated. The variation of total heat loss with the area ratio for different inclination of the receiver is shown in Fig. 12. The quantity of air trapped inside the receiver increases with the area ratio. The high stagnant air zone reduces the convection currents. The radiation heat loss decreases with the increasing the area ratio. The total heat loss from the receiver was reduced sharply for very high area ratios ($A_w/A_1 > 8$) and very low area ratios ($A_w/A_1 < 4$). It was observed that the marginal drop in total heat loss for the area ratios between 4 and 8. The receiver with the area ratios up to 4 involved significant heat losses. Therefore, it is advisable to operate the receiver with higher area ratios ($\geqslant$10). However, at higher area ratios, the solar radiation intercepted (reflected from the dish concentrator) by the aperture plane of the receiver is reduced. For the better performance of the receiver, it is recommended to have an area ratio of 8.

The total heat loss from the receiver has been estimated for operating temperatures varying from 300 °C to 700 °C. The variation of total heat loss with operating temperature for different orientations of the receiver is shown in Fig. 13. The combined convection and radiation heat loss increases with the receiver operating temperatures. The effect of angle of inclination on total heat loss is more significant for higher receiver temperature, whereas it is less significant at lower receiver temperature.

Table 3
Combined convection and radiative heat losses

Inclination angle	Area ratio (A_w/A_1)	Convection heat loss (W)	Radiation heat loss (W)	Total heat loss (W)
0	2	435.06	559.11	994.17
	4	286.41	291.72	578.13
	8	220.54	302.56	424.10
	10	136.02	119.38	255.40
30°	2	404.11	559.11	963.22
	4	269.25	291.72	560.97
	8	214.63	203.56	418.19
	10	130.32	119.38	249.71
60°	2	325.20	559.11	884.32
	4	229.39	291.72	521.11
	8	186.50	203.56	390.06
	10	114.21	119.38	233.59
90°	2	190.59	559.11	749.70
	4	163.49	291.72	465.20
	8	139.83	203.56	343.39
	10	89.41	119.38	208.79

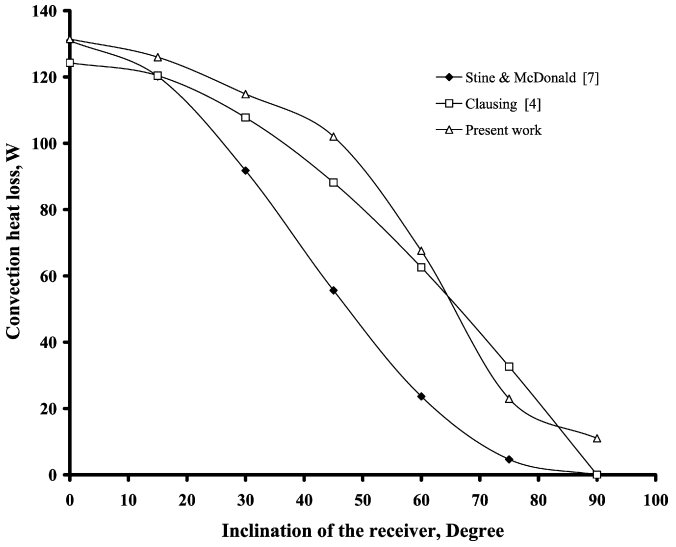

Fig. 14. Comparison of modified cavity receiver at 400 °C with other heat loss models.

5. Comparison of present model with other heat loss models

The convection heat loss model for modified cavity receiver with $A_w/A_1 = 8$ is compared with well known convection heat loss models such as Clausing [4] and Stine and McDonald [7]. These models were proposed with an assumption that the receivers have negligible natural convective heat loss at 90° inclination. Nevertheless there is a possibility of existing convection between the inner surface of the cavity and ambient. In the present model, heat loss at 90° has been considered for accurate determination of total heat loss. The comparison of modified cavity receiver with other heat loss models at 400 °C is shown in Fig. 14. It is observed that the present 2D convection heat loss model is comparable with Clausing [4] and Stine and McDonald [7] models. It is evident that the deviation is primarily due to nature of the geometry of the receiver and the characteristics length. It is also evident that these models were based on the specific receiver geometry.

6. Conclusions

A 2D numerical analysis of combined laminar natural convection and surface radiation in the modified cavity receiver of a solar dish was presented. Two separate Nusselt numbers were proposed for both natural convection and surface radiation. The incorporation of the radiation in a modified cavity receiver completely alters the heat loss rate. It was found that the convective loss was significantly influenced by the orientation of the receiver. The convection heat loss was dominated by the radiation heat loss for higher receiver inclination angle (>45°). The radiation heat loss was considerably influenced by the area ratios. The receiver showed better performance at an area ratio of 8. The model may effectively be used to estimate the convection and radiation heat losses from the cavity receiver of solar parabolic dish collector system. The accuracy of the combined natural convection and surface radiation heat loss estimations of modified cavity receiver may be improved by incorporating 3D effects.

References

[1] S. Yasuaki, K. Fujimura, T. Kunugi, N. Akino, Natural convection in a hemispherical enclosure heated from below, Int. J. Heat Mass Transfer 37 (1999) 1605–1617.
[2] J.M. Khubeiz, E. Radziemska, W.M. Lewandowski, Natural convective heat transfer from an isothermal horizontal hemispherical cavity, Appl. Energy 73 (2002) 261–275.
[3] W.M. Lewandowski, P. Kubski, J.M. Khubeiz, H. Bieszk, T. Wilczewski, S. Szymanski, Theoretical and experimental study of natural convection heat transfer from isothermal hemisphere, Int. J. Heat Mass Transfer 40 (1997) 101–109.
[4] A.M. Clausing, An analysis of convective losses from cavity solar central receiver, Solar Energy 27 (1981) 295–300.
[5] P. LeQuere, F. Penot, M. Mirenayat, Experimental study of heat loss through natural convection from an isothermal cubic open cavity, Sandia Laboratory Report, 1981, SAND81-8014.
[6] D.L. Siebers, J.S. Kraabel, Estimating convective energy losses from solar central receivers, Sandia Laboratory Report, 1984, SAND84-8717.
[7] C.G. McDonald, Heat loss from an open cavity, Sandia Laboratory Report, 1995, SAND95-2939.
[8] U. Leibfried, J. Ortjohann, Convective heat loss from upward and downward-facing cavity receivers: Measurements and calculations, ASME J. Solar Energy Eng. 117 (1995) 75–84.
[9] T. Taumoefolau, S. Paitoonsurikarn, G. Hughes, K. Lovegrove, Experimental investigation of natural convection heat loss from a model solar concentrator cavity receiver, ASME J. Solar Energy Eng. 126 (2004) 801–807.
[10] S. Paitoonsurikarn, K. Lovegrove, A new correlation for predicting the free convection loss from solar dish concentrating receivers, in: Proceedings of 44th ANZSES conference, 2006, 01-09, Australia.
[11] N. Sendhil Kumar, K.S. Reddy, Comparison of receivers for solar dish collector system, Energy Conversion and Management (2007), doi: 10.1016/j.enconman.2007.07.026, in press.
[12] N. Sendhil Kumar, K.S. Reddy, Numerical investigation of natural convection heat loss in modified cavity receiver for fuzzy focal solar dish concentrator, Solar Energy 81 (2007) 846–855.

[13] J.L. Lage, J.S. Lim, A. Bejan, Natural convection with radiation in a cavity with open top end, ASME J. Heat Transfer 114 (1992) 479–486.
[14] C.X. Lin, S.Y. Ko, M.D. Xin, Effects of surface radiation on turbulent free convection in an open-ended cavity, Int. Comm. Heat Mass Transfer 21 (1994) 117–129.
[15] C. Balaji, S.P. Venkateshan, Interaction of radiation with free convection in an open cavity, Int. J. Heat Fluid Flow 15 (4) (1994) 317–324.
[16] C. Balaji, S.P. Venkateshan, Combined conduction, convection and radiation in a slot, Int. J. Heat Fluid Flow 16 (1995) 139–144.
[17] A.A. Dehghan, M. Behnia, Combined natural convection–conduction and radiation heat transfer in a discretely heated open cavity, ASME J. Heat Transfer 118 (1996) 56–64.
[18] N. Ramesh, W. Merzkirch, Combined convective and radiative heat transfers in side-vented open cavity, Int. J. Heat Fluid Flow 22 (2001) 180–187.
[19] S.N. Singh, S.P. Venkateshan, Numerical study of natural convection with surface radiation in side-vented open cavities, Int. J. Thermal Sci. 43 (4) (2004) 865–876.
[20] J.F. Hinojosa, R.E. Cabanillas, G. Alvarez, C.E. Estrada, Nusselt number for the natural convection and surface thermal radiation in a square tilted open cavity, Int. Comm. Heat Mass Transfer 32 (2005) 1184–1192.
[21] H. Bouali, A. Mezrhab, H. Amaoui, M. Bouzidi, Radiation—natural convection heat transfer in an inclined rectangular enclosure, Int. J. Thermal Sci. 45 (2006) 553–566.
[22] C. Balaji, S.P. Venkateshan, Correlations for free convection and surface radiation in a square cavity, Int. J. Heat Fluid Flow 15 (3) (1994) 249–251.
[23] N. Sendhil Kumar, K.S. Reddy, Study of combined natural convection and surface radiation in a modified cavity receiver for solar parabolic dish collector, in: Proceedings of the 1st National Conference on Advances in Energy Research, AER-2006, IITB, Macmillan, New Delhi, 2006, pp. 157–163.
[24] S.W. Yuan, Foundations of Fluid Mechanics, third ed., Prentice-Hall International Inc., London, 1988, pp. 104–113.
[25] R. Siegel, J. Howell, Thermal Radiation Heat Transfer, fourth ed., Taylor & Francis, New York, 2002.